Crystalline Phase in the Ultrahigh Molecular-Weight Polyethylene Gel Solution and Xerogel

P. M. Pakhomov,[1] Svetlana Khizhnyak,[1] H. Reuter,[2] A. Tshmel[3]

[1]*Physico-Chemistry Department, Tver' State University, 170002 Tver', Russia*
[2]*University Osnabrueck, Barbara str. 7, D-49069 Osnabrueck, Germany*
[3]*Fracture Physics Department, Ioffe Physico-Technical Institute, Russian Academy of Sciences, 194021 St. Petersburg, Russia*

Received 7 May 2002; accepted 24 October 2002

ABSTRACT: The transverse and longitudinal sizes of crystallites in thermoreversible polyethylene gels and xerogels were measured using wide-angle X-ray scattering and a low-frequency Raman spectroscopy, and were found to be 10–40 and 4–5 nm, respectively. The experimental data evidence the imperfection of primary crystallites in both dimensions. The gel-to-solid transition results in gaining the direct interaction between crystalline entities with increasing the cracking, on the one hand, and forming the clusters of stacked crystalline platelets linked with regular molecular rods, on the other hand. These contact interaction leads, in addition, to the coiling of a great part of regular sequences that emanate from the crystallite cores to the amorphous region. © 2003 Wiley Periodicals, Inc. J Appl Polym Sci 89: 373–378, 2003

INTRODUCTION

Crystallization history of gel-derived semicrystalline polymers starts from the formation of tiny lamellar crystals in gel solution.[1] In ultrahigh molecular-weight polyethylene (UHMWPE), the thickness of such primary crystallites was estimated as 3 to 5 nm in dependence of the solution used.[2,3] The first stage of the polymer gel processing directed to produce a high-performance material is the removal of solvent with collapsing the liquid-saturated substance to xerogel preform. On the supermolecular level, this procedure is characterized by the gel-to-solid transformation that disturbs a metastable equilibrium existing in gel solution and creates the structural units inherent in solid polymers.

This communication presents the wide-angle X-ray scattering (WAXS) and low-frequency Raman data revealing some particular features of the crystalline phase in the solidifying UHMWPE gel. A combination of these techniques allowed us to measure the changes in transverse crystal dimensions and to determine not only the longitudinal crystal size but also detect the presence of the straight chain segments (SCS) whose lengths exceed significantly the crystal thickness.

Correspondence to: A. Tshmel (chmel@mail.ioffe.ru).

Journal of Applied Polymer Science, Vol. 89, 373–378 (2003)

SAMPLES AND EQUIPMENT

The samples were made of UHMWPE ($M_W = 1.7 \times 10^6$) soluted in paraffin oil. The 3 wt % suspensions of the polymer powder were placed in a cylindrical flask and slowly heated from 20 to 180°C with intensive stirring. A hot UHMWPE solution was poured into a glass Petri plate. The rapid cooling resulted in gel formation what was concluded from arising turbidity of the solvent and supported by rheological tests performed at 60°C with the help of a rotary viscometer Carri-Med CSL 100.

The gels were released from the solvent and shaped to xerogel films of ~200 μm thick. To remove the low-volatile paraffin oil, a preform was repeatedly squeezed between sheets of filter paper in a hand press. This mode of solidifying of gels was chosen to exclude the recrystallization process that could be expected in the case of application of the gel drying procedure.

The WAXS experiments were performed on a STADI P STOE & CIE X-ray diffractometer using a monochromatic $\lambda = 1.54$ Å radiation. The Raman spectra were recorded on a triple monochromator DILOR XY 800 equipped with a Spectra Physics 100 mW NdYVO4 laser.

RESULTS

WAXS

The experimental WAXS patterns from a gel solution and a solvent-free xerogel in the range up to $2\theta = 25°$

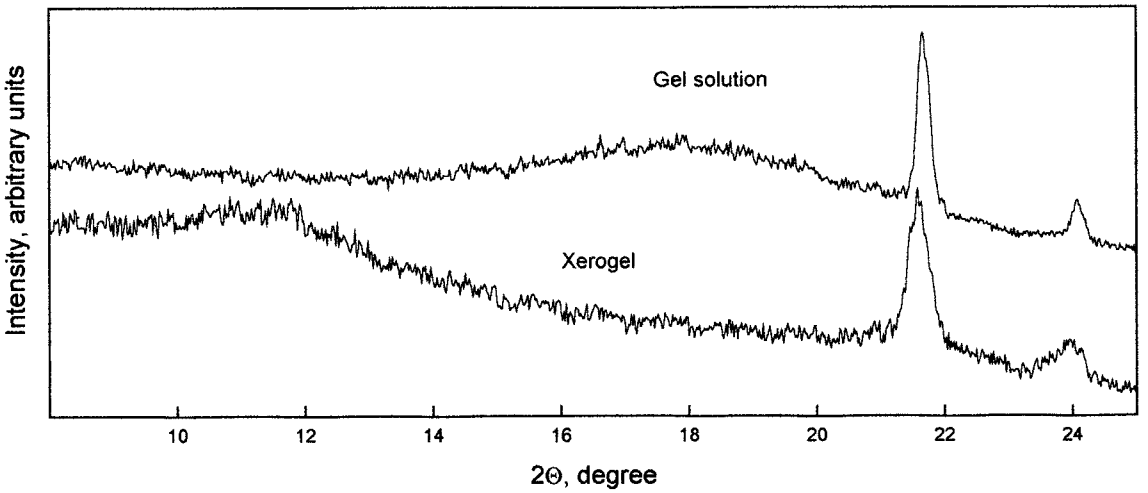

Figure 1 WAXS curves for UHMWPE gel solution (a) and xerogel (b).

are shown in Figure 1. The solvent removal leads to the decrease of the integral intensity of the amorphous halo due to reduced contribution of the scattering from the irregular phase. Regarding the crystalline components, even the overview spectra allow one to detect visually an asymmetry in the equatorial diffraction peaks [110] and [200]. The asymmetry is hardly noticeable in the spectrum of the gel solution, but the effect becomes persistent with removing the solvent: in the spectrum of xerogel, the [200] peak at ~24° exhibits a clearly seen small-angle shoulder.

The peak asymmetry is caused by the deviation of a certain number of unit cells from their canonical orthorhombic configuration in view of the presence of defect sites in crystallites or the imperfection of some crystallites in whole.[4] The difference in the asymmetry between two detected equatorial peaks is caused by the difference in the response of planes (110) and (200) to the crystal deformation. The low-angle character of the skew in the scattering profile evidences the presence of enlarged interchain spacings in defect sites.[5]

To estimate the individual contribution of unresolved peaks, we applied the deconvolution procedure developed in ref. 6 for asymmetric X-ray scattering curves (Figs. 2 and 3). The experimental diffraction peaks [200] in the WAXS spectra of gel solution and solid xerogel were corrected for the background scattering, and then each corrected curve was approximated by two Gaussian components. The resulted profiles demonstrate good fitting to the experimental patterns. The calculated parameters of the components are given in Table I.

Angular positions of the maxima of the crystalline components are determined by the cell parameters a_i (here, i is the conventional number of the component, see Fig. 2) in accordance with the basic relation:

$$2a_i = m\lambda / \sin\Theta_{[200]}{}^{(i)}. \quad (1)$$

Here, m is the diffraction order; in our case $m = 2$.

The values a_i found from eq. (1) are collected in Table II, together with the transverse crystallite dimensions (L_i) calculated using the Debye-Scherrer formula:

$$L_i = K\lambda / \beta \cos\Theta_{[200]}{}^{(i)} \quad (2)$$

where $K = 0.94$ is the constant; β is the peak halfwidth measured in radians. As ascribing to every Gaussian component a specific value of L_i, we imply indirectly that two sorts of unit cells belong to crystalline domains differing in transverse size. The longitudinal characterization of the crystallites was obtained from the Raman studies.

LAM

In contrast to the small-angle X-ray scattering technique, which is usually applied for the determination of the thickness of crystallites, the low-frequency Raman spectroscopy gives the length distribution of all regular rods in the sample but not only those that involved into the crystalline phase. This is a certain advantage in the case of presence of significant contribution of "noncrystalline" regular structure (in terms of ref. 7), because this allows one to detect the *all-trans* sequences whose length is not equal to the crystal thickness.

The light scattering on the accordion-like longitudinal acoustic modes (LAM) localized on the SCS produces a band situated in the vicinity of the central line of the spontaneous Raman scattering. The SCS length distribution is available from the appropriate treatment of the LAM band intensity profile.

Figure 4(a) and (b) shows the Raman spectra of the UHMWPE gel solution and solid xerogel, respectively. (The logarithmic scale for the Raman intensity, I, was

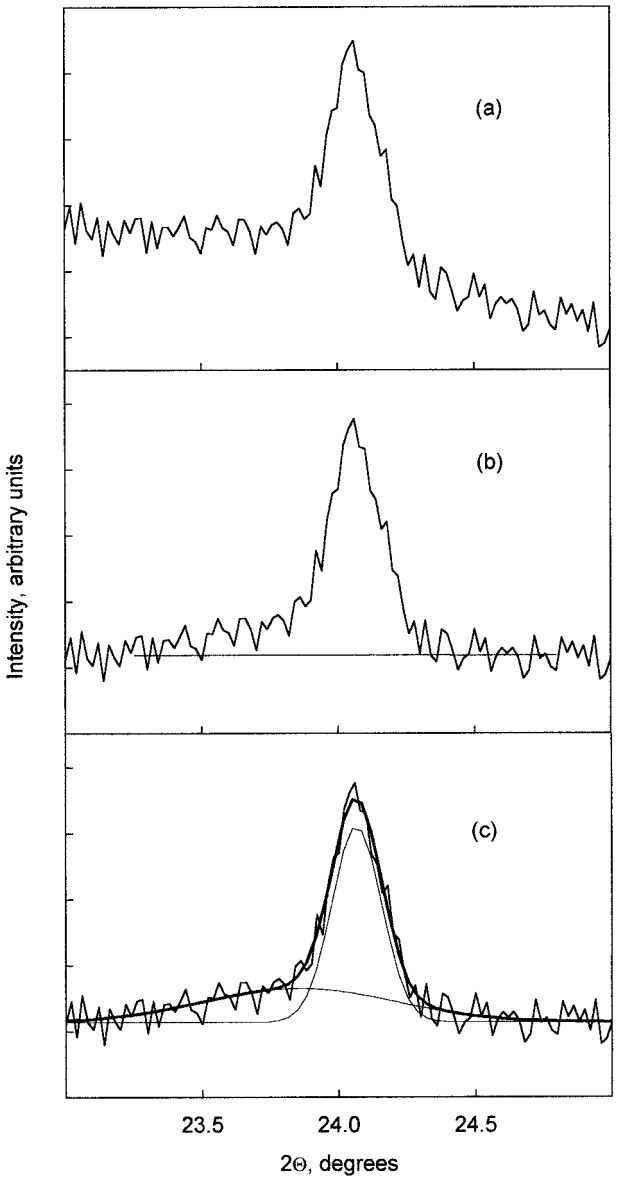

Figure 2 The experimental (a), corrected for the background (b), and deconvoluted in Gaussian components (c) WAXS profile in the range of the [200] diffraction peak from a gel solution.

chosen to enhance the details of the low-amplitude portion of the spectra). The molecular weight (MW) fraction of the SCS of length l is given by the function $G_{MW}(l)$, which corresponds to the Raman intensity $I(\omega)$ as:[8]

$$G_{MW}(l) \propto n(\omega)\omega_1^2 \mathrm{I}(\omega) l, \qquad (3)$$

where $n(\omega) = 1 - \exp(-hc\omega/kT)$ is the Boltzmann factor, ω_l is the frequency of acoustic vibrations of the *all-trans* sequence that determines the Raman shift in dependence of the value of l:

$$\omega_l = (2cl)^{-1}(E/\rho)^{1/2} \qquad (4)$$

Here, c is the speed of light; ρ is the density; E is the Young's modulus in the chain direction.

The MW distributions of the SCS over lengths, computed using eq. (3) and eq. (4), are shown in Figure 4(c) and (d). The position of maximum in each distribution corresponds to the most probable length of the ordered stems (l_{pro}), that should be (in the case of a perfect crystal) close to the average crystal thickness (l_c). In an ill-ordered system, such as a crystalline phase in the gel solution, l_{pro} is to some extent higher than l_c owing to the contribution of unfolded chains entering the interface zone from the crystal core surface. A noticeable asymmetry of the SCS length distribution with a long tail extending to $l > l_{pro}$ indicates the imperfect geometry of the basal planes in crystallites. After removal of the solvent, the value l_{pro} decreases from 51 Å to 43 Å (Table II), and the function $G_{MW}(l)$ becomes much narrower and obviously bimodal. This means, first, the smoothing of the crystal surface in result of coiling the portions of the SCS that quit the crystallite cores normally their surface. Second, a weak-amplitude peak at ~170 Å evidences the formation of some quantity of SCS whose lengths is a few times more than the longitudinal size of the crystallites (i.e., 43 Å, in supposition $l_c \approx l_{pro}$ that is justified by the small $G_{MW}(l)$ halfwidth in the xerogel). In view of the uniformity of the thermal prehistory of the material, one cannot ascribe these "long" ordered stems to the SCS in crystallites of other thickness. On the other hand, the arising of a well-pronounced extra peak in the SCS length distribution points out the existence of a particular dimension in the structure.

Such "quantum" dimensions can arise in result of the penetration of some SCS into adjacent crystallites with formation of regular sequences similar to taut-tie molecules in oriented structures. In this case, a peak corresponding to stems linking two crystals (whose position should be at $l = l_c \times 2 + \delta$, where δ is the

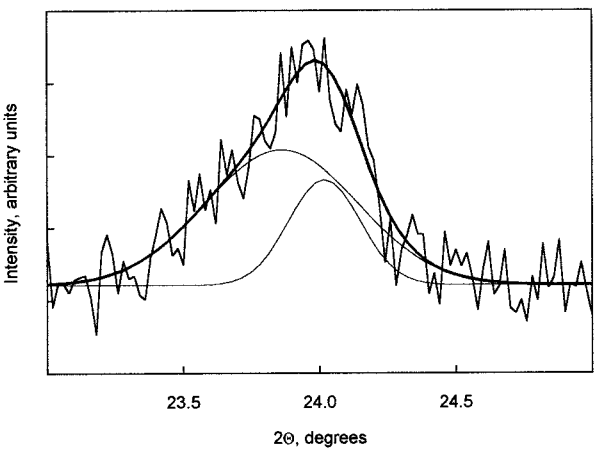

Figure 3 The corrected for the background scattering and deconvoluted in Gaussian components WAXS profile in the range of the [200] diffraction peak from a xerogel.

TABLE I
Angular Position and Halfwidth of the Diffraction Peak from Planes (200) in UHMWPE Gels

Sample	$2\Theta_1$	$2\Delta\Theta_1$	$2\Theta_2$	$2\Delta\Theta_2$
Gel solution	24.06 ± 0.01	0.69 ± 0.02	23.85 ± 0.05	0.18 ± 0.02
Solid xerogel	24.03 ± 0.02	0.52 ± 0.03	23.84 ± 0.04	0.27 ± 0.03

length of two intercrystallite spacers, or $43 \times 2 + \delta$) is overlapped by the main dome. Therefore, the isolated peak at 170 Å belongs to the stems involved in three closely arranged folded crystals: $170 = 43 \times 3 + 2\delta$.

DISCUSSION

The main diffraction peak [200] ($i = 1$) at $2\Theta \approx 24°$ in both convoluted WAXS spectra is corresponded to "ordinary" orthorhombic unit cells whose parameter a_1 (equal to 7.39 Å and 7.40 Å in gel solutions and xerogels, respectively) is close to the "standard" value 7.41 Å given in a monography.[9] The peak at lower 2Θ ($i = 2$) could be regarded as an effective representation of the contribution of "defect" cells with dimensions a_2 other than a_1. The areas under the Gaussian components correspond to the weight fractions of the unit cells of two sorts (i.e., differing in the value of a).

When comparing the deconvoluted spectra of the gel solution and xerogel, one can see that despite the intensity perturbation in the X-ray pattern in result of the gel-to-solid transition, the diffraction peak positions of both components change insignificantly. This, of course, is an expectable fact for the peak at ~24° related to undistorted cells, but the coincidence of the positions of the peaks introduced independently in a formalistic way is quite surpassingly. We conclude that the extra peaks at $2\Theta \cong 23.85°$ in liquid and solid gel phases are due to the scattering on the (200) planes in particular structural defects. Among possible steric defects capable to affect the unit cell parameters, Davis and coworkers[4] called those that originate from the fold interaction, the difference in fold planes, and from the crystal site distortion in molecular domains of all kinds. We suppose that in our case of the ill-ordered structure, the defects of fold packing in crystallites should be regarded as the principal cause of the bimodal cell dimension distribution.

This approach would be in good agreement with the Keller model[1] of the gel state (where the folded-chain platelets immersed in the solvent are connected to each other by flexible links) if one admit that these crystalline platelets have substantial defects in the fold packing that affect the regular diffraction pattern (Fig. 5). The defects of this kind one should expect in mosaic crystallites, in particular, those that cracked with incomplete separation of broken parts. The disturbance of regular folding along the adjacent (connected) edges of the crystallite parts must cause the molecular strain of tensile character with gaining the diffraction intensity at $2\theta < 2\theta_1$. The amount of distorted sites grows with removing the solvent in result of the compression-induced interaction between crystallites during the sample squeezing.

Regarding the longitudinal crystal size, this characteristic must remain unchanged because the solvent was removed from the gel solution without a heat treatment. However, in result of the gel-to-solid transformation the structure becomes much more compacted. Some lamellar crystallites enter in close contact with forming a kind of "sandwiches" with equally oriented (complanar) fold planes [Fig. 5(b)]. These stacked platelets are linked by the intercrystallite $l > 2l_c$ regular stems presented by an individual peak in the SCS length distribution [Fig. 4(b)].

This mechanism of the fold doubling was first put forward by Keller and coworkers[10–12] to explain some trends observed when annealing PE single crystals and solution-crystallized polyamides. "Quantum" increase of the crystal size was explained by penetration of folds from one lamella into adjacent lamella in results of chain sliding through the interface [Fig. 5(c)]. More recently, this model was applied by Rastogy and coworkers[13] to interpret the LAM data obtained in experiments on melting the gel-derived PE samples. Dreyfuss and Keller[11] stressed, that the folds

TABLE II
Some Dimensional Characteristics of the Crystalline Phase in UHMWPE Gels (Å)

Sample	a_1	a_2	L_1	L_2	l_{pro}
Gel solution	7.39 ± 0.01	7.43 ± 0.02	470 ± 20	120 ± 10	51 ± 1
Solid xerogel	7.40 ± 0.01	7.44 ± 0.01	310 ± 30	160 ± 20	43 ± 1[a]

[a] Here $l_{pro} \approx l_c$, see text.

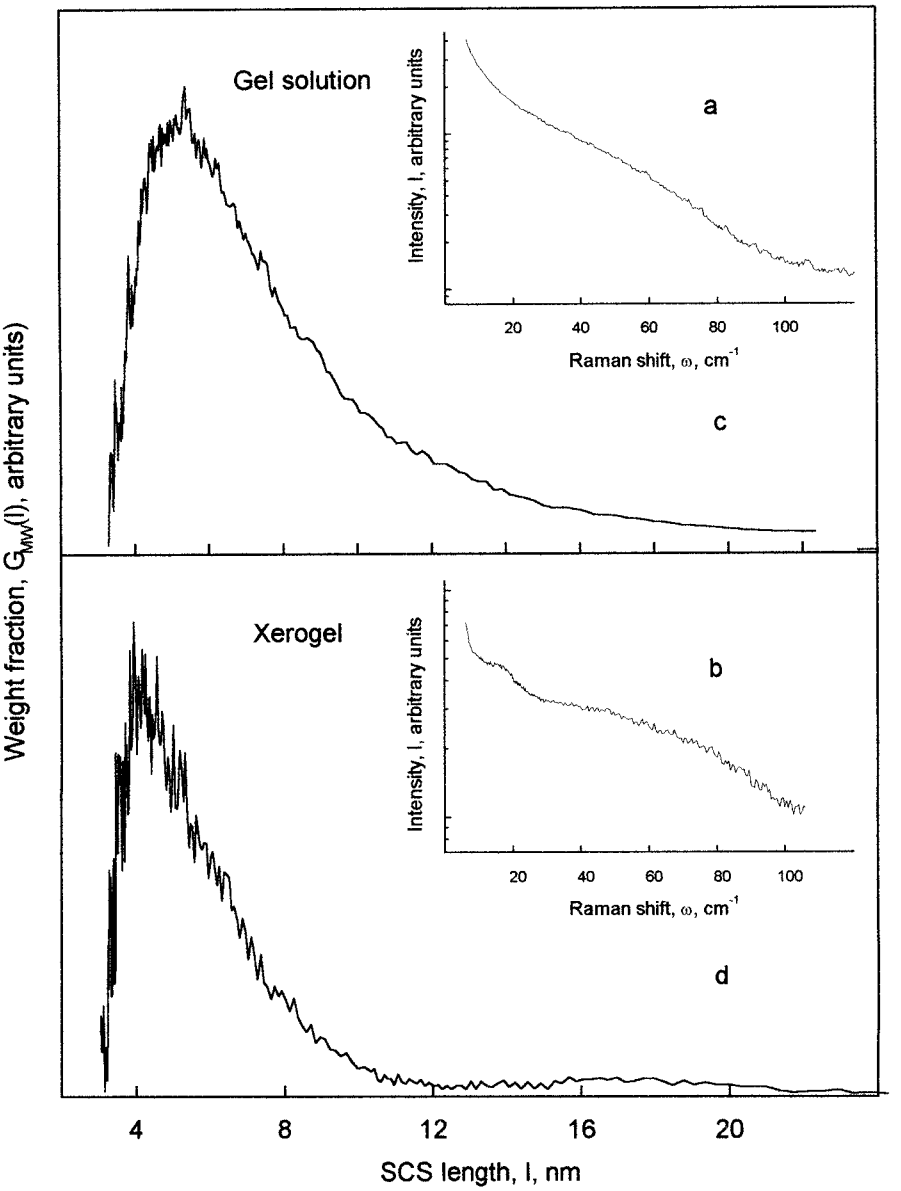

Figure 4 The experimental Raman spectra in the range of the LAM bands for the gel solution (a) and xerogel (b) served as original data for calculation of the SCS length distributions in the gel solution (c) and xerogel (d).

in the intermediate state (i.e., those of $l_c < l < 2\,l_c$) are unstable in principle; therefore, the doubling compensates the "missing" SCS within the defect crystallites. The thermodynamic driving force that causes the chains to slide is related with the necessity to minimize the surface free energy under particular conditions.[10]

CONCLUSION

The LAM (low-frequency Raman) spectroscopy indicates the presence of tiny (~50 Å) crystallites in the UHMWPE gel solution whose basal planes are quite imperfect. In result of the gel-to-solid transformation, a great part of the unfolded SCS extending from the crystallite cores to the interface zones become coiled thus smoothing the fold surfaces; at the same time, there appear clusters consisting of two to three complanar lamellar crystals in compacted xerogels.

The WAXS data evidence a mosaic structure of crystallites in the UHMWPE gel and xerogel. This does not contradict a widely accepted model of crystalline phase in polymer gel solution as an ensemble of crystalline domains linked by tortuous chains,[1] but demonstrates a high degree of defectness of the individual crystalline entities. Keller[1] argued for high drawability of the gel-derived polymers due to their tenuous and mobil molecular network. The quasi-mosaic structure of primary crystallites is an additional factor facilitat-

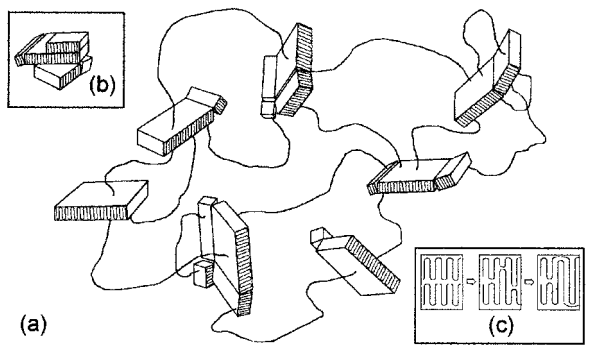

Figure 5 (a) A schematic representation of the Keller model[1] modified in accordance with the actual WAXS data. (b) Stacked crystalline platelets formed in result of the compression-induced gel-to-solid transformation. (c) A schematic model used in ref. 12 to explain the doubling phenomenon in the stacked adjacent lamellae.

ing the rearrangement of crystalline entities to the highly oriented structure.

The authors are pleased to thank Lyuba Myasnikova for her interest to this work and pointed remarks.

References

1. Keller, A. Faraday Discuss 1995, 101, 1.
2. Kober, K.; Khizhnyak, S.; Pakhomov, P.; Tshmel, A. J Appl Polym Sci 1999, 72, 1795.
3. Pakhomov, P. M.; Khizhnyak, S.; Ruhl, E.; Egorov, V.; Tshmel, A. European Polym J 2003, 39, 1019.
4. Davis G. T.; Weeks J. J.; Martin G. M.; Eby R. K. J Appl Phys 1974, 45, 4175.
5. Baker, A. M. E.; Windle, A. H. Polymer 2001, 42, 667.
6. Marikhin, V. A. Doctor of Science Thesis, Ioffe Physico-Technical Institute, Leningrad, 1991.
7. Fu, Y.; Chen, W.; Pyda, M.; Londono, D.; Annis, B.; Boller, A.; Habenschuss, A.; Cheng, J.; Wunderlich, B. Macromol Sci Phys 1996, B35, 37.
8. Snyder, R. G.; Krause, S. J.; Scherer, J. R. Polym Sci Phys Ed 1978, 16, 1593.
9. Geil, P. H. Polymer Single Crystals; Interscience Publishers, A Division of John Wiley & Sons: New York, 1963.
10. Dreyfuss, P.; Keller, A. J Macromol Sci Phys 1970, 20 811.
11. Dreyfuss, P.; Keller, A. J Polym Sci B 1970, 8, 3.
12. Bahram, P. J.; Keller, A. J Polym Sci Phys Ed 1989, 27, 1029.
13. Rastogi, S.; Spoelstra, A. B.; Goossens, J. G. P.; Lemstra, P. J. Macromolecules 1997, 30, 7880.